



Comprehensive imaging of cortical networks

Simon Peron, Tsai-Wen Chen and Karel Svoboda

Neural computations are implemented by activity in spatially distributed neural circuits. Cellular imaging fills a unique niche in linking activity of specific types of neurons to behavior, over spatial scales spanning single neurons to entire brain regions, and temporal scales from milliseconds to months. Imaging may soon make it possible to track activity of all neurons in a brain region, such as a cortical column. We review recent methodological advances that facilitate optical imaging of neuronal populations *in vivo*, with an emphasis on calcium imaging using protein indicators in mice. We point out areas that are particularly ripe for future developments.

Address

Janelia Research Campus, HHMI, Ashburn VA 20147, United States

Corresponding author: Svoboda, Karel (svobodak@janelia.hhmi.org)

Current Opinion in Neurobiology 2015, **32**:115–123

This review comes from a themed issue on **Large-scale recording technology**

Edited by **Francesco Battaglia** and **Mark J Schnitzer**

<http://dx.doi.org/10.1016/j.conb.2015.03.016>

959-4388/© 2015 Published by Elsevier Ltd.

Introduction

A fundamental question in neuroscience is how information relevant to behavior is processed in neural circuits. Even the simplest perceptual behaviors engage thousands of neurons across multiple regions of cortex [1,2]. In contrast, typical electrophysiological studies sample only a handful of neurons in a single brain area [3]. Moreover, the type of neuron recorded and its position within the neural circuit are typically unknown [4] and long-term recording from the same neurons is inefficient [5]. As a result, the dynamics of neural circuits during behavior and learning are poorly understood.

Over the last decade, cellular calcium imaging has become widely used to image activity in neuronal populations [6]. In most neurons, action potentials (APs) are tightly coupled to large (20-fold) and rapid (rise time, 1 millisecond) increases in intracellular free calcium concentration, which can be used to read out neural activity [7–9]. Calcium imaging samples activity of all neurons in an imaging volume [10] and can readily be combined with visualization of cell type markers to analyze activity in

specific nodes of neural circuits [11–15]. With genetically encoded calcium indicators, activity in the same neuronal populations has been imaged across days and weeks [16,17[•],18,19^{••}].

Calcium imaging is now routinely used to measure the spatial organization of receptive fields [10,20,21] and to provide a relatively unbiased view of behavior-related activity in populations of neurons [13,22]. Calcium imaging efficiently samples activity in relatively rare cell types [11] and measures changes in neural coding during learning [17[•],18,19^{••},23,24].

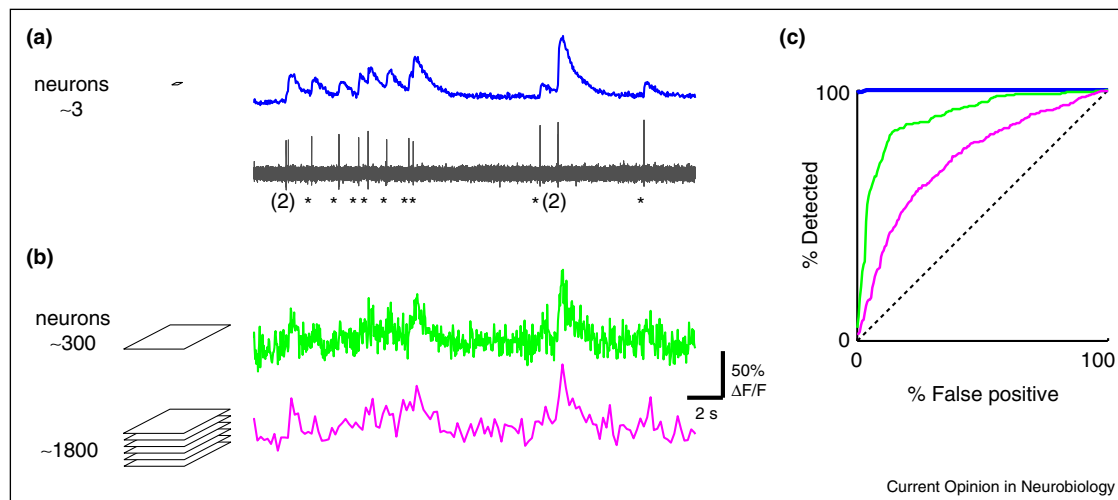
The majority of studies still image only dozens to hundreds of neurons at a time. Here we review the challenges faced by attempts to produce comprehensive activity maps based on large-scale imaging. Our focus is on studies with single cell resolution based on two-photon laser scanning microscopy (TPLSM) in behaving head-fixed mice.

Fluorescent probes for neuronal function

The rapid development of protein sensors for neuronal function has been a major driver of new applications for imaging *in vivo*. In the past, experimenters had to choose between sensitive small-molecule sensors, which need to be loaded into brain tissue using invasive chemical methods [25], and less sensitive protein sensors, which can be delivered using the versatile tools of molecular genetics [26]. Recent efforts in protein engineering [16,27^{••},28[•],29,30^{••}] have boosted the sensitivity of GECIs, allowing them to largely supplant synthetic indicators for imaging neuronal populations. Under favorable conditions, new GECIs detect single action potentials (APs) in the intact brain [27^{••}] (Figure 1a).

Despite these advances, compared to electrophysiology calcium imaging still has several drawbacks. Existing GECIs are not sufficiently sensitive to detect low levels of activity in some cell types, such as parvalbumin-positive interneurons [27^{••}]. The performance degrades as the per-neuron sampling time declines (Figure 1b,c). Furthermore, calcium sensors are slow compared to the precision in neural spike trains [27^{••},29], limiting the insights that can be drawn about spike timing in neural coding [31,32] and connectivity in neural circuits [33]. Imaging is confined to optically accessible structures, typically less than one millimeter from the surface of the brain or an optical implant (e.g. endoscope). In contrast, electrophysiology has excellent signal-to-noise ratio, dynamic range, time resolution, and spatial reach.

Figure 1



Action potential detectability in imaging experiments. **(a)** GCaMP6s signal (blue, top) and extracellular spikes (black, bottom; single spikes correspond to asterisks) recorded from a single neuron (data from Ref. [27]). The size of the field of view (FOV, 30 μm square) corresponded to approximately three cortical neurons, imaged at 30 Hz. **(b)** Simulations of different imaging conditions based on the data from panel A assuming identical laser power. Green, approximately 300 neurons imaged at 30 Hz. The signal-to-noise ratio is smaller compared to (a) because the signal is distributed across a larger number of neurons. Magenta, approximately 1800 neurons imaged at 5 Hz. **(c)** Single action potential detection probability as a function of false positive rate for isolate single spike events (ROC curve; colors corresponding to a, b). The ability to detect single action potentials deteriorates as the number of simultaneously imaged neurons increases. In experiments in behaving animals many other factors further degrade detectability, including movement noise, increased fluorescence baseline at higher spike rates, and uncertainty about spike timing.

For these reasons calcium imaging currently occupies a niche complementary to electrophysiology.

Improvements in protein sensors will continue to drive advances in population imaging. For example, even more sensitive GECIs would expand the range of cell types amenable to calcium imaging and increase the number of neurons that can be imaged simultaneously. Given that the brightness of state-of-the-art GECIs is already high [27], improvements in signal-to-noise ratio will mainly be driven by increasing the fluorescence change upon calcium binding [34,35]. The most obvious path to better detectability is thus to engineer GECIs with zero resting fluorescence and higher affinity for calcium. Red-shifted GECIs will enable imaging deeper in tissue [36].

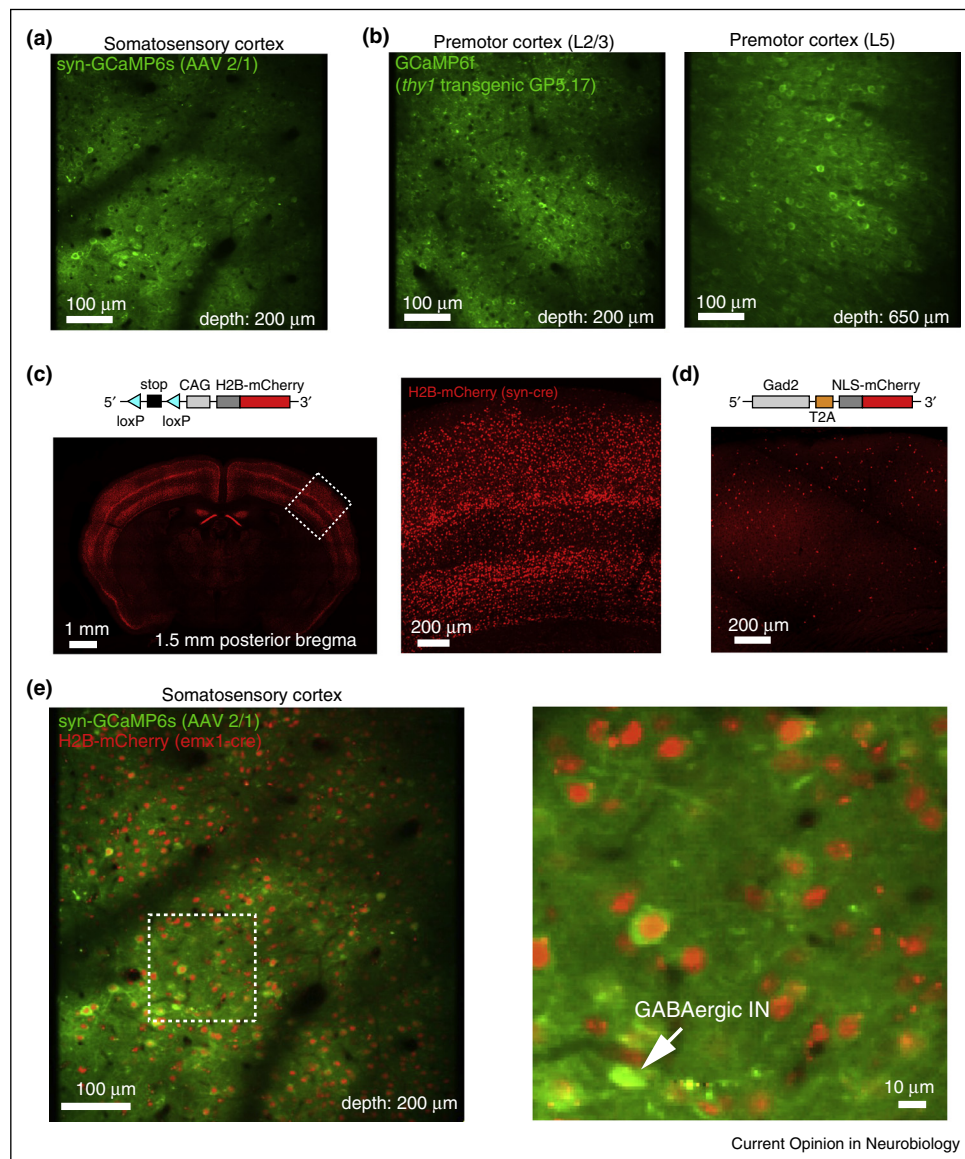
Protein sensors for state variables other than calcium could overcome some of the limitations of calcium imaging for measuring population activity. In particular, protein voltage sensors can be much faster than calcium sensors [37]. But despite recent improvements, their sensitivity for detecting activity at the level of single neurons is still substantially inferior to protein calcium sensors [38–41]. The best-of-class calcium indicators change fluorescence up to 50-fold during physiological changes in intracellular calcium, whereas voltage sensors change less than 2-fold for typical voltage changes. Fundamental biological constraints provide additional challenges for voltage imaging. Calcium can be sensed by molecules distributed

throughout the neuronal cytoplasm. Typical expression levels (50 μM) [17,42] correspond to approximately 10^7 fluorescent molecules in the soma, sufficient to produce a bright signal. In contrast, voltage needs to be sensed across the lipid bilayer, and many fewer fluorescent proteins can be incorporated into the two-dimensional membrane (a typical density for membrane proteins, $10 \mu\text{m}^{-2}$, corresponds to 10^4 molecules in the somatic membrane). Intracellular fluorescence contributed by sensors in the endoplasmic reticulum produces non-productive background. Orders of magnitude improvements will be required to make voltage sensors competitive with GECIs for imaging of neuronal populations at cellular resolution.

Gene delivery methods

In the mammalian brain, stable long-term expression of protein sensors for imaging remains challenging. Adeno-associated viruses (AAVs) and other viral vectors can produce the high intracellular GECI concentrations, typically 10–100 μM [17,42], required for *in vivo* imaging [16,43] (Figure 2a). However, concentrations vary across neurons, within a cell type, and across cell types [19]. Expression levels continue to rise over months until they cause aberrant cell health [16,27], limiting the window for GECI imaging to a few weeks, depending on the promoter construct, viral titer, injection volume, type of GECI and other factors. Viral gene transfer also requires challenging surgeries. Best-practice procedures demand

Figure 2



Methods for transgene expression for *in vivo* imaging. **(a)** *In vivo* TPLSM image from a mouse infected with AAV2/1-syn-GCaMP6s in the somatosensory cortex. **(b)** *In vivo* TPLSM images of transgenic expression of GCaMP6f in a thy-1 transgenic mouse (GP5.17, JAX 025393). Left, L2/3; right, L5. **(c)** Transgenic nuclear expression of mCherry. The Cre reporter mouse (R26-LSL-H2B-mCherry; [19], JAX 023139) was crossed to a synapsin-Cre transgenic mouse. Left, coronal section, showing dense expression of mCherry-H2B in the neocortex. Right, blow-up of the somatosensory cortex. **(d)** Expression of nuclear localized mCherry in GABAergic neurons in Gad2 knock-in mice (Gad2-t2A-NLS-mCherry; [19], JAX 023140). **(e)** *In vivo* TPLSM image in an LSL-CAG-H2B-mCherry X emx1-Cre mouse, with AAV2/1-syn-GCaMP6s infection (green). The mCherry expression is restricted to excitatory neurons in cortex, whereas GCaMP6s expression is pan-neuronal. The green GCaMP6 fluorescence in many neurons is low and indistinct with respect to the fluorescent neuropil. The high-contrast images of the red nuclei aid in movement correction, image segmentation, and cell-type specific analysis (white arrow points to a GABAergic interneuron).

tiny injection volumes (5–50 nl) [17,19], which can result in variable numbers of infected cells and inhomogeneous expression levels.

In transgenic mice, GECIs can be expressed at constant levels over many months, without any signs of cytotoxicity [42,44,45,46] (Figure 2b). Expression is reproducible across neurons and individual mice, without invasive

surgeries. However, established schemes for flexible reporter expression (e.g. GCaMP3 driven by the CAG promoter targeted to the *Rosa26* gene locus) [47] fail to provide adequate expression levels for cellular *in vivo* imaging [42]. Expression under the *Thy1* promoter [44] is sufficiently high in some mouse lines. But the labeling patterns depend on transgene cassette integration site and differ in an unpredictable manner across lines.

Selected individual mouse lines typically serve specific narrow purposes. In addition, expression is limited to excitatory neurons.

A promising new strategy is based on a docking site in the transcriptionally permissive TIGRE locus, in combination with τ TA-based transcriptional amplification. In this scheme, transgene expression is driven from the tetracycline response element in a cre-dependent manner. Expression of GECIs and other probes can be substantially higher compared to Rosa26-CAG based reporters, sufficient for *in vivo* imaging [48**].

Because the fluorescence change upon calcium binding is a key factor in determining the sensitivity of molecular calcium sensors [34,35], the most sensitive GECIs have low resting fluorescence [27**]. This can make neurons difficult to visualize and segment in the absence of activity (Figure 2a,b). Co-expression of a fluorescent protein with non-overlapping fluorescence emission can address this problem [19**]. Transgenic mice with mCherry [49] targeted to the nuclei of specific cell types can be combined with GECI expression for *in vivo* imaging (Figure 2c–e) [19**]. The red nuclear protein aids segmentation of neurons, movement correction, image alignment across days, and cell-type specific analysis, greatly facilitating *in vivo* imaging.

Microscopy methods

The vast majority of cellular *in vivo* imaging studies have been performed using 2-photon laser scanning microscopy [50]. 2-Photon excitation provides localization of excitation in scattering tissue, which in turn produces three-dimensional contrast and resolution. As a result of localization of excitation, scattered and non-scattered photons both contribute to signal. This greatly boosts the image contrast and signal-to-noise ratio compared to wide-field microscopy, particularly when imaging in scattering media [51].

The principles of 2-photon excitation microscopy demand that individual excitation volumes (on the order of $1\ \mu\text{m}^3$) are sampled sequentially. The sampling rate is ultimately limited by the fluorescence lifetime of typical fluorophores (3 ns for GFP) [52], which is comparable to the inter-pulse interval for commonly used pulsed light sources (10 ns) [53]. It is therefore in principle possible to sample a cortical column ($300\ \mu\text{m} \times 300\ \mu\text{m} \times 1000\ \mu\text{m}$) with its 10^4 neurons at 10 Hz (100 imaging planes, separated by $10\ \mu\text{m}$, 10 ns/voxel). Two factors currently conspire to make this target unachievable by a factor of ten or more. First, scanning methods (e.g. resonant scanners) are too slow and inefficient. Second, under acceptable illumination conditions and expression levels, best-of-class GECIs are not sufficiently sensitive. Improvements in laser scanning technology (e.g. [54,55]) and GECI

performance should make imaging of entire cortical columns with single cell resolution achievable.

Penetration depth of TPLSM is limited by scattering and absorption. TPLSM imaging up to 1 mm deep has been demonstrated [51]. Deeper brain regions can be accessed by removing intervening brain tissue [22,56] or by insertion of endoscopes [57,58] or prisms [59] into the brain regions of interest.

A variety of wave front shaping methods have been proposed to overcome sample-induced aberrations, such as spherical aberrations and astigmatism [60,61,62*]. These methods can dramatically improve signal levels for small structures that are on the order of or smaller than the two-photon excitation volume, such as spines and axons, but have more modest effects on images of larger structures [62*]. Wave front engineering can also correct for strong local scattering with large improvements in signal level at depth [63*]; however, these corrections have to be recomputed for every few micrometers of sample, making this method too slow for most applications.

A promising direction for deep imaging is based on longer wavelength fluorophores. Red and near-IR fluorescence emission is absorbed less by blood [64], yielding improved signal collection when imaging *in vivo*. Furthermore, longer excitation wavelengths are scattered less on the way into the tissue [65]. The penetration depth is therefore significantly better for red and near-IR fluorophores [36*]. Red GECIs with properties comparable to the best green GECIs are on the horizon [66**,67**] and poised to boost the penetration depth of TPLSM imaging significantly.

Three-photon fluorescence excitation has been demonstrated for deep imaging [68]. However, three-photon cross-sections are tiny. As a result very high peak intensities and long pixel dwell times are required for practical image formation. Three-photon excitation microscopy is thus currently too slow for physiological imaging. The high peak intensities required to drive three-photon excitation may also cause rapid photobleaching of the fluorophores and other types of destructive photochemistry [69].

Serial sampling limits the speed of TPLSM. Spurred by new fast and sensitive solid state cameras, wide-field microscopy [70*], light-field microscopy [71], and light-sheet microscopy [72] have been used to measure neural activity in rodents. Compared to TPLSM, scattering and out-of-focus fluorescence rapidly degrade signal and contrast with imaging depth. However, many orders of magnitude more fluorescence is collected simultaneously, and computational methods can potentially overcome some of the signal degradation. In advantageous situations, such as brain areas with sparse activity patterns in space and

time, quasi two-dimensional structures, and sparse labeling, it may be possible to extract signals corresponding to activity of individual neurons [70[•]]. In optically clear preparations such as the zebrafish, these approaches have allowed sampling of activity across the entire brain [71,73]. An important goal is to establish the correspondence between fluorescence dynamics extracted from these data and neural activity in individual neurons, as has been done for TPLSM [25,27^{••},28[•],74,75].

From images to spikes

Imaging experiments produce stacks of images. Extracting quantitative and robust estimates of spike trains or time-varying spike rate is a complex computational problem.

The biophysics of calcium imaging implies that no data analysis trick will provide error-free spike trains. Furthermore, the performance of any algorithm depends on many factors relating to imaging conditions (Figure 1b,c). Even the spike rate of individual neurons matters. For neurons firing at very low rates, false-positive spikes may build to become a substantial fraction of the total detected events. At high firing rates, the elevated baseline fluorescence decreases detection due to larger shot noise and reduced sensitivity if the indicator approaches saturation. We still need a better understanding of the factors underlying sensitivity and dynamic range of calcium imaging.

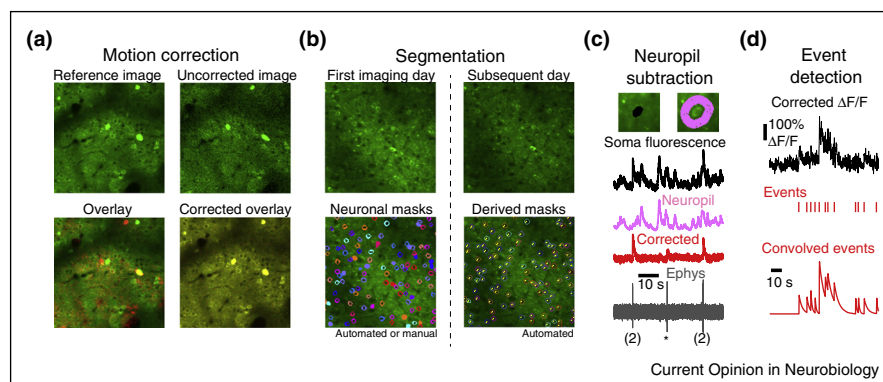
Extracting quantitative estimates of spike trains or time-varying spike rate from raw images involves multiple complex steps. Low-level analysis starts with movement correction (Figure 3a). Lateral motion usually dominates [76] and algorithms for correcting lateral motion are

relatively mature [76,77[•],78]. Axial motion correction is computationally expensive and necessitates sampling multiple planes [12]. Methods for closed-loop motion correction may ultimately become necessary.

Segmentation involves separating the signal corresponding to individual neurons from the signal of other neurons and the neuropil [12,27^{••},75,79[•],80] (Figure 3b,c). The neuropil signal arises from fluorophore expressed in unresolved small dendrites and axons [75], as well as out-of-focus fluorescence. Regions of interest (ROIs) can be drawn using either morphological [19^{••},27^{••},78], or activity-based [79[•],80] algorithms. Whereas morphological approaches are computationally light and potentially unbiased with respect to activity (e.g., when based on structural red nuclear markers [19^{••}]), activity-based approaches can in principle yield more accurate ROI boundaries. A hybrid approach, where morphology-seeded ROIs are refined using activity-based approaches, may be optimal.

Following ROI selection, neuropil contamination must be corrected for. This problem is especially acute when GECIs are confined to the cytoplasm (a relatively thin shell around the nucleus). Because of the limited resolution of 2-photon microscopy *in vivo*, especially axially [81], the neuropil signal substantially bleeds into the somatic signal [27^{••},81], so that $F_{\text{measured}} = \alpha F_{\text{neuropil}} + \beta F_{\text{soma}}$. The contamination α depends on the point spread function (PSF) and neuronal geometry. Assuming an idealized PSF (Gaussian with $SD_{x,y} = 0.3 \mu\text{m}$ and $SD_z = 3 \mu\text{m}$) and neuron geometry ($2 \mu\text{m}$ thick shell surrounding an $8 \mu\text{m}$ diameter nucleus) implies $\alpha = 0.3\text{--}0.5$. Empirically we determined $\alpha = 0.7\text{--}1$ to be most effective for removing

Figure 3



Data processing pipeline for imaging data. **(a)** Motion correction is carried out by aligning images from one imaging session to a reference image, collected during an epoch of low motion. In the bottom panels, the reference image is shown in red, whereas the image being corrected is green. **(b)** Image segmentation involves separating the regions of interest (e.g. individual somata) from the rest of the image. Once an image has been segmented, algorithms can relocate the same neurons on subsequent imaging sessions (right). Segmentation is critical for extracting fluorescence dynamics corresponding to individual neurons. **(c)** Subtracting the local neuropil signal from the contaminated somatic signal reveals the actual somatic response. Loose-seal recordings were adapted from [27^{••}]. **(d)** Event detection from the fluorescence dynamics of individual neurons. This provides an estimate of the timing of rapid increases in activity. Events are convolved with their respective amplitudes and decay time constants to produce a de-noised $\Delta F/F$ trace.

neuropil associated fluorescence contamination (Figure 3c; [19^{••},27^{••}]). This large value for α suggests that out-of-focus fluorescence is more pronounced than expected from PSF measurements [81]. Since the neuropil signal is not spatially uniform (e.g., in mouse somatosensory cortex, neuropil pixel correlation λ is approximately 150 μm) a local neuropil estimate must be employed (Figure 3c) [19^{••}]. The importance of neuropil correction is readily apparent in experiments combining imaging with electrophysiology ([27^{••}]; Figure 3c).

Fluorescence change in ROIs is often reported as neural ‘activity’. However, fluorescence is a non-linear function of intracellular free calcium [28[•]], which in turn is a non-linear function of the recent activity of the neuron [82]. This implies that calcium imaging-based ‘tuning’ curves of individual neurons are distorted [83] (Figure 4a,b).

The complex relationship between fluorescence dynamics and activity (Figure 4c) makes explicit spike inference desirable (Figure 3d). Most researchers use deconvolution or template matching (e.g. [14,23,84,85,86[•],87]). These algorithms do not explicitly account for the non-linear coupling between spikes and fluorescence changes. Because neurons exhibit diverse spike-to-fluorescence transfer functions, one set of parameters will only be effective for a subset of cells. Future spike inference algorithms will have to employ nonlinear transfer functions and need to use neuron-specific parameters derived from fluorescence dynamics alone.

Compared to the rapid advances in experimental methods, computational analysis of imaging data remains in its

infancy. Currently used methods are *ad hoc*, slow, poorly documented, and differ across labs, implying that hard-won experimental data are underutilized. A lack of standardization hinders reproducibility and comparison across studies. Moreover, with increasing imaging speeds, data sets have ballooned. A resonant scanning TPLSM produces approximately 100 GB of data per experiment-hour. Nearly complete automation and modern computational methods, such as distributed computing [88[•]] will have to supplant the semi-manual methods in use today to fully exploit the richness of these datasets.

A principled approach for analysis of imaging data must start with quantitative comparisons of analysis algorithms. This could be achieved in challenges, where computational approaches are evaluated against datasets with ground truth, which are now publicly available (simultaneously detected spikes using electrophysiology [27^{••}]: <http://dx.doi.org/10.6080/K02R3PMN>; segmentation based on structural fluorescence markers [19^{••}], e.g. Figure 2c–e: <http://dx.doi.org/10.6080/K0TB14TN>). Benchmarking should be performed in an open-source environment that supports cluster and distributed computing [89]. Benchmarking would stimulate the development of new algorithms and wide adoption of best-of-class methods.

Once spike trains or spike rates have been extracted, they can be mined for insight into the neural mechanisms underlying behavior. The general goal is to relate the activity patterns of neuronal populations to animal behavior. The technical challenges of high-dimensional data analysis are shared with other types of neurophysiology data [90] and are beyond the scope of this review.

Figure 4

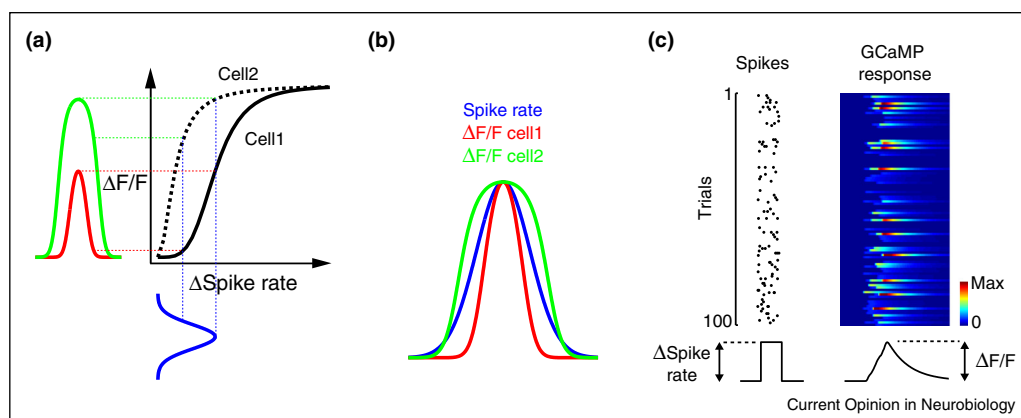


Illustration of potential biases introduced by calcium imaging. **(a)** Response curves for two hypothetical neurons experiencing an identical change in spike rate but having distinct spike-fluorescence transfer functions. At baseline Cell 2 is closer to saturation than Cell 1. This could be because of higher baseline activity or resting calcium concentration. Identical changes in spike rate (blue) would translate into different fluorescence change in Cell 1 (red) and Cell 2 (green). **(b)** The true tuning curve of both cells (spike rate, blue) produces distinct and distorted fluorescence tuning curves (Cell 1, red; Cell 2, green). **(c)** Simulated Poisson spikes (left) and fluorescence transients based on data in [27^{••}]. Simply using $\Delta F/F$ yields a temporally distorted mean response across trials, which deconvolution or spike estimation can ameliorate.

Outlook: towards mesoscale imaging of neural networks

We are on the verge of a new kind of neurophysiology, bridging the gap between single neurons and brain areas. We recently demonstrated comprehensive measurement of behavior-related activity in the superficial layers of several cortical columns, producing a neural activity map comprising more than 10,000 neurons per animal [19**]. Microscopy schemes are in place to image multiple brain regions simultaneously [91*,92]. It will soon be possible to track activity of all neurons in a brain region and measure the interactions between populations in multiple brain areas.

We expect further improvements in proteins sensors to continue to drive advances in population imaging. More sensitive GECIs will facilitate imaging larger number of neurons simultaneously. Faster kinetics will allow estimates of spike trains over a larger range of spike rates. Red-shifted indicators will expand the range of imaging depths. Automation and standardization of image analysis pipelines will be critical to deal with the resulting big data deluge and to convert image data to neuronal state variables.

Conflict of interest statement

Nothing declared.

Acknowledgements

We thank Jeremy Freeman, Na Ji, Aaron Kerlin and Zengcai Guo for comments on the manuscript.

References and recommended reading

Papers of particular interest, published within the period of review, have been highlighted as:

- of special interest
- of outstanding interest

1. Romo R, de Lafuente V: **Conversion of sensory signals into perceptions, memories and decisions.** *Prog Neurobiol* 2013, **103**:41-75.
2. Guo ZV, Li N, Huber D, Ophir E, Gutnisky DA, Ting JT, Feng G, Svoboda K: **Flow of cortical activity underlying a tactile decision in mice.** *Neuron* 2014, **81**:179-194.
3. Stevenson IH, Kording KP: **How advances in neural recording affect data analysis.** *Nat Neurosci* 2011, **14**:139-142.
4. O'Connor DH, Huber D, Svoboda K: **Reverse engineering the mouse brain.** *Nature* 2009, **461**:923-929.
5. Tolia AS, Ecker AS, Siapas AG, Hoenselaar A, Keliris GA, Logothetis NK: **Recording chronically from the same neurons in awake, behaving primates.** *J Neurophysiol* 2007, **98**:3780-3790.
6. Grienberger C, Konnerth A: **Imaging calcium in neurons.** *Neuron* 2012, **73**:862-885.
7. Baker PF, Hodgkin AL, Ridgway EB: **Depolarization and calcium entry in squid giant axons.** *J Physiol* 1971, **218**:709-755.
8. Jaffe DB, Johnston D, Lasser RN, Lisman JE, Miyakawa H, Ross WN: **The spread of Na⁺ spikes determines the pattern of dendritic Ca²⁺ entry into hippocampal neurons.** *Nature* 1992, **357**:244-246.
9. Svoboda K, Denk W, Kleinfeld D, Tank DW: **In vivo dendritic calcium dynamics in neocortical pyramidal neurons.** *Nature* 1997, **385**:161-165.
10. Ohki K, Chung S, Kara P, Hubener M, Bonhoeffer T, Reid RC: **Highly ordered arrangement of single neurons in orientation pinwheels.** *Nature* 2006, **442**:925-928.
11. Fu Y, Tucciarone JM, Espinosa JS, Sheng N, Darcy DP, Nicoll RA, Huang ZJ, Stryker MP: **A cortical circuit for gain control by behavioral state.** *Cell* 2014, **156**:1139-1152.
12. Kerlin AM, Andermann ML, Berezovskii VK, Reid RC: **Broadly tuned response properties of diverse inhibitory neuron subtypes in mouse visual cortex.** *Neuron* 2010, **67**:858-871.
13. O'Connor DH, Peron SP, Huber D, Svoboda K: **Neural activity in barrel cortex underlying vibrissa-based object localization in mice.** *Neuron* 2010, **67**:1048-1061.
14. Sato TR, Svoboda K: **The functional properties of barrel cortex neurons projecting to the primary motor cortex.** *J Neurosci* 2010, **30**:4256-4260.
15. Chen JL, Carta S, Soldado-Magraner J, Schneider BL, Helmchen F: **Behaviour-dependent recruitment of long-range projection neurons in somatosensory cortex.** *Nature* 2013, **499**:336-340.
16. Tian L, Hires SA, Mao T, Huber D, Chiappe ME, Chalasani SH, Petreanu L, Akerboom J, McKinney SA, Schreiner ER, Bargmann CI et al.: **Imaging neural activity in worms, flies and mice with improved GCaMP calcium indicators.** *Nat Methods* 2009, **6**:875-881.
17. Huber D, Gutnisky DA, Peron S, O'Connor DH, Wiegert JS, Tian L, Oertner TG, Looger LL, Svoboda K: **Multiple dynamic representations in the motor cortex during sensorimotor learning.** *Nature* 2012, **484**:473-478.
- The first paper demonstrating long-term imaging of neural populations during learning, here a tactile decision task. Ensembles of motor cortex neurons change their selectivity and timing with respect to behavioral events during learning.
18. Peters AJ, Chen SX, Komiyama T: **Emergence of reproducible spatiotemporal activity during motor learning.** *Nature* 2014, **510**:263-267.
19. Peron S, Freeman J, Iyer V, Guo C, Svoboda K: **A cellular resolution map of barrel cortex activity during tactile behavior.** *Neuron* 2015, **86** in press.
- Comprehensive sampling of behavior-related activity in all neurons of the superficial layers of the mouse somatosensory cortex during tactile behavior.
20. Issa JB, Haeffele BD, Agarwal A, Bergles DE, Young ED, Yue DT: **Multiscale optical Ca(2+) imaging of tonal organization in mouse auditory cortex.** *Neuron* 2014, **83**:944-959.
21. Bonin V, Histed MH, Yurgenson S, Reid RC: **Local diversity and fine-scale organization of receptive fields in mouse visual cortex.** *J Neurosci* 2011, **31**:18506-18521.
22. Dombeck DA, Harvey CD, Tian L, Looger LL, Tank DW: **Functional imaging of hippocampal place cells at cellular resolution during virtual navigation.** *Nat Neurosci* 2010, **13**:1433-1440.
23. Komiyama T, Sato TR, O'Connor DH, Zhang YX, Huber D, Hooks BM, Gabitto M, Svoboda K: **Learning-related fine-scale specificity imaged in motor cortex circuits of behaving mice.** *Nature* 2010, **464**:1182-1186.
24. Margolis DJ, Lütcke H, Schulz K, Haiss F, Weber B, Kügler S, Hasan MT, Helmchen F: **Reorganization of cortical population activity imaged throughout long-term sensory deprivation.** *Nat Neurosci* 2012, **15**:1539-1546.
25. Stosiek C, Garaschuk O, Holthoff K, Konnerth A: **In vivo two-photon calcium imaging of neuronal networks.** *Proc Natl Acad Sci USA* 2003, **100**:7319-7324.
26. Kerr R, Lev-Ram V, Baird G, Vincent P, Tsien RY, Schafer WR: **Optical imaging of calcium transients in neurons and pharyngeal muscle of C. elegans.** *Neuron* 2000, **26**:583-594.
27. Chen TW, Wardill TJ, Sun Y, Pulver SR, Renninger SL, Baohan A, Schreiner ER, Kerr RA, Orger MB, Jayaraman V, Looger LL et al.: **Ultrasensitive fluorescent proteins for imaging neuronal activity.** *Nature* 2013, **499**:295-300.

Introduces the GCaMP6 family of green GECIs, optimized for *in vivo* imaging of neural activity and demonstrates several use cases for GCaMP6, including activity of neural populations and single synapses. GCaMP6 is the current standard in the field.

28. Akerboom J, Chen TW, Wardill TJ, Tian L, Marvin JS, Mutlu S, Calderon NC, Esposti F, Borghuis BG, Sun XR, Gordus A *et al.*: **Optimization of a gcamp calcium indicator for neural activity imaging.** *J Neurosci: Off J Soc Neurosci* 2012, **32**:13819-13840.
Compares spiking and GCaMP5 fluorescence changes in the same neurons *in vivo*. The nonlinear relationship between fluorescence dynamics and activity causes a higher variability in the fluorescence response compared to the spiking response.
29. Horikawa K, Yamada Y, Matsuda T, Kobayashi K, Hashimoto M, Matsu-ura T, Miyawaki A, Michikawa T, Mikoshiba K, Nagai T: **Spontaneous network activity visualized by ultrasensitive Ca(2+) indicators, yellow cameleon-nano.** *Nat Methods* 2010, **7**:729-732.
30. Zhao Y, Araki S, Wu J, Teramoto T, Chang YF, Nakano M, Abdelfattah AS, Fujiwara M, Ishihara T, Nagai T, Campbell RE: **An expanded palette of genetically encoded Ca(2) indicators.** *Science* 2011, **333**:1888-1891;

Akerboom J, Carreras Calderon N, Tian L, Wabnig S, Prigge M, Tolo J, Gordus A, Orger MB, Severi KE, Macklin JJ *et al.*: **Genetically encoded calcium indicators for multi-color neural activity imaging and combination with optogenetics.** *Front Mol Neurosci* 2013, **6**:2.
This pair of papers reports the first red GECIs with robust fluorescence changes upon calcium binding.
31. O'Connor DH, Hires SA, Guo ZV, Li N, Yu J, Sun QQ, Huber D, Svoboda K: **Neural coding during active somatosensation revealed using illusory touch.** *Nat Neurosci* 2013, **16**:958-965.
32. Gollisch T, Meister M: **Rapid neural coding in the retina with relative spike latencies.** *Science* 2008, **319**:1108-1111.
33. Fujisawa S, Amarasingham A, Harrison MT, Buzsaki G: **Behavior-dependent short-term assembly dynamics in the medial prefrontal cortex.** *Nat Neurosci* 2008, **11**:823-833.
34. Yasuda R, Nimchinsky EA, Scheuss V, Pologruto TA, Oertner TG, Sabatini BL, Svoboda K: **Imaging calcium concentration dynamics in small neuronal compartments.** *Sci STKE* 2004, **2004** pl5.
35. Wilt BA, Fitzgerald JE, Schnitzer MJ: **Photon shot noise limits on optical detection of neuronal spikes and estimation of spike timing.** *Biophys J* 2013, **104**:51-62.
36. Kobat D, Horton NG, Xu C: **In vivo two-photon microscopy to 1.6-mm depth in mouse cortex.** *J Biomed Opt* 2011, **16**:106014.
Demonstrates enhanced penetration depth for two-photon imaging using 1280 nm excitation light and far red fluorophores.
37. Knopfel T: **Genetically encoded optical indicators for the analysis of neuronal circuits.** *Nat Rev Neurosci* 2012, **13**:687-700.
38. Kralj JM, Douglass AD, Hochbaum DR, Maclaurin D, Cohen AE: **Optical recording of action potentials in mammalian neurons using a microbial rhodopsin.** *Nat Methods* 2012, **9**:90-95.
39. Gong Y, Wagner MJ, Zhong Li J, Schnitzer MJ: **Imaging neural spiking in brain tissue using FRET-opsin protein voltage sensors.** *Nat Commun* 2014, **5**:3674.
40. Jin L, Han Z, Platasa J, Woollorton JR, Cohen LB, Pieribone VA: **Single action potentials and subthreshold electrical events imaged in neurons with a fluorescent protein voltage probe.** *Neuron* 2012, **75**:779-785.
41. Zou P, Zhao Y, Douglass AD, Hochbaum DR, Brinks D, Werley CA, Harrison DJ, Campbell RE, Cohen AE: **Bright and fast multicoloured voltage reporters via electrochromic fret.** *Nat Commun* 2014, **5**:4625.
42. Zariwala HA, Borghuis BG, Hoogland TM, Madisen L, Tian L, De Zeeuw CI, Zeng H, Looger LL, Svoboda K, Chen TW: **A CRE-dependent GCaMP3 reporter mouse for neuronal imaging in vivo.** *J Neurosci: Off J Soc Neurosci* 2012, **32**:3131-3141.

43. Wallace DJ, Zum Alten Borgloh SM, Astori S, Yang Y, Bausen M, Kugler S, Palmer AE, Tsien RY, Sprengel R, Kerr JN, Denk W *et al.*: **Single-spike detection in vitro and in vivo with a genetic Ca(2+) sensor.** *Nat Methods* 2008, **5**:797-804.
44. Dana H, Chen T-W, Hu A, Shields BC, Guo C, Looger L, Kim D, Svoboda K: **Thy1-gcamp6 transgenic mice for neuronal population imaging in vivo.** *PLoS ONE* 2014, **9**:e108697.
Reports the first transgenic mice expressing the GCaMP6 family of indicators, driven by the thy-1 promoter. Different lines have distinct expression patterns. GP5.17 and GP4.3 are especially useful.
45. Drenth S, Mues M, Micale V, Wotjak CT, Dietzel S, Schubert M, Scharr A, Hassan S, Wahl-Schott C, Biel M, Krishnamoorthy G *et al.*: **Biocompatibility of a genetically encoded calcium indicator in a transgenic mouse model.** *Nat Commun* 2012, **3**:1031.
46. Chen Q, Cichon J, Wang W, Qiu L, Lee S-JR, Campbell NR, DeStefino N, Goard MJ, Fu Z, Yasuda R, Looger LL *et al.*: **Imaging neural activity using thy1-gcamp transgenic mice.** *Neuron* 2012, **76**:297-308.
47. Madisen L, Mao T, Koch H, Zhuo JM, Berenyi A, Fujisawa S, Hsu YW, Garcia AJ 3rd, Gu X, Zanella S, Kidney J *et al.*: **A toolbox of cre-dependent optogenetic transgenic mice for light-induced activation and silencing.** *Nat Neurosci* 2012, **15**:793-802.
48. Madisen L *et al.*: **Transgenic mice for intersectional targeting of neural sensors and effectors with high specificity and performance.** *Neuron* 2015, **85**:942-958.
A new strategy for reporter expression in mice that is well-matched for *in vivo* imaging applications. Reports dozens of new transgenic mouse lines for *in vivo* imaging and optogenetics.
49. Shaner NC, Campbell RE, Steinbach PA, Giepmans BN, Palmer AE, Tsien RY: **Improved monomeric red, orange and yellow fluorescent proteins derived from *Drosophila* sp. red fluorescent protein.** *Nat Biotechnol* 2004, **22**:1567-1572.
50. Denk W, Svoboda K: **Photon upmanship: why multiphoton imaging is more than a gimmick.** *Neuron* 1997, **18**:351-357.
51. Helmchen F, Denk W: **Deep tissue two-photon microscopy.** *Nat Methods* 2005, **2**:932-940.
52. Yasuda R, Harvey CD, Zhong H, Sobczyk A, van Aelst L, Svoboda K: **Supersensitive ras activation in dendrites and spines revealed by two-photon fluorescence lifetime imaging.** *Nat Neurosci* 2006, **9**:283-291.
53. Cheng A, Goncalves JT, Golshani P, Arisaka K, Portera-Cailliau C: **Simultaneous two-photon calcium imaging at different depths with spatiotemporal multiplexing.** *Nat Methods* 2011, **8**:139-142.
54. Katona G, Szalay G, Maak P, Kaszas A, Veress M, Hillier D, Chiovini B, Vizi ES, Roska B, Rozsa B: **Fast two-photon in vivo imaging with three-dimensional random-access scanning in large tissue volumes.** *Nat Methods* 2012, **9**:201-208.
55. Duemani Reddy G, Kelleher K, Fink R, Saggau P: **Three-dimensional random access multiphoton microscopy for functional imaging of neuronal activity.** *Nat Neurosci* 2008, **11**:713-720.
56. Mizrahi A, Crowley JC, Shtoyerman E, Katz LC: **High-resolution in vivo imaging of hippocampal dendrites and spines.** *J Neurosci* 2004, **24**:3147-3151.
57. Levene MJ, Dombeck DA, Kasischke KA, Molloy RP, Webb WW: **In vivo multiphoton microscopy of deep brain tissue.** *J Neurophysiol* 2004, **91**:1908-1912.
58. Flusberg BA, Cocker ED, Piyawattanametha W, Jung JC, Cheung EL, Schnitzer MJ: **Fiber-optic fluorescence imaging.** *Nat Methods* 2005, **2**:941-950.
59. Andermann ML, Gilfoy NB, Goldey GJ, Sachdev RN, Wolfel M, McCormick DA, Reid RC, Levene MJ: **Chronic cellular imaging of entire cortical columns in awake mice using micropipettes.** *Neuron* 2013, **80**:900-913.
60. Rueckel M, Mack-Bucher JA, Denk W: **Adaptive wavefront correction in two-photon microscopy using coherence-gated wavefront sensing.** *Proc Natl Acad Sci USA* 2006, **103**:17137-17142.

61. Ji N, Milkie DE, Betzig E: **Adaptive optics via pupil segmentation for high-resolution imaging in biological tissues.** *Nat Methods* 2010, **7**:141-147.
62. Wang C, Liu R, Milkie DE, Sun W, Tan Z, Kerlin A, Chen TW, Kim DS, Ji N: **Multiplexed aberration measurement for deep tissue imaging in vivo.** *Nat Methods* 2014, **11**:1037-1040.
Reports a new method for aberration measurement and correction in tissue. Demonstrates diffraction-limited imaging of small structures in the mouse brain *in vivo*. One correction applies over a large tissue volume.
63. Tang J, Germain RN, Cui M: **Superpenetration optical microscopy by iterative multiphoton adaptive compensation technique.** *Proc Natl Acad Sci USA* 2012, **109**:8434-8439.
Use of high-speed MEMS mirrors to correct for strong light scattering deep in neural tissue. The procedure can enhance signal levels by orders of magnitude, but only in a small part of the tissue volume.
64. Svoboda K, Block SM: **Biological applications of optical forces.** *Ann Rev Biophys Biomol Struct* 1994, **23**:247-285.
65. Oheim M, Beaupre E, Chaigneau E, Mertz J, Chappak S: **Two-photon microscopy in brain tissue: parameters influencing the imaging depth.** *J Neurosci Methods* 2001, **111**:29-37.
66. Dana H, Sun Y, Hasseman JP, Tsegaye G, Holt GT, Fosque BF, Schreier ER, Brenowitz SD, Jayaraman V, Looger LL, Svoboda K *et al.*: **"Improved red fluorescent genetically-encoded calcium indicators for in vivo imaging" (that's the title of the submitted abstract, eventually we changed it on the poster to: "Improved red protein indicators for in vivo calcium imaging")**. *SfN Abstract* 2014.
These two reports [66*,67**] introduce improved red GECIs for *in vivo* imaging based on multiple distinct protein scaffolds.
67. Inoue M, Takeuchi A, Horigane S, Ohkura M, Gengyo-Ando K, Fujii H, Kamiyo S, Takemoto-Kimura S, Kano M, Nakai J, Kitamura K *et al.*: **Rational design of a high-affinity, fast, red calcium indicator R-CAMP2.** *Nat Methods* 2015, **12**:64-70.
See annotation to Ref. [66**].
68. Horton NG, Wang K, Kobat D, Clark CG, Wise FW, Schaffer CB, Xu C: **Three-photon microscopy of subcortical structures within an intact mouse brain.** *Nat Photon* 2013, **7**.
69. Patterson GH, Piston DW: **Photobleaching in two-photon excitation microscopy.** *Biophys J* 2000, **78**:2159-2162.
70. Ziv Y, Burns LD, Cocker ED, Hamel EO, Ghosh KK, Kitch LJ, El Gamal A, Schnitzer MJ: **Long-term dynamics of CA1 hippocampal place codes.** *Nat Neurosci* 2013, **16**:264-266.
Reports wide field imaging of neural populations in the CA1 region of the hippocampus in freely moving mice. Localized fluorescence transients are consistent with place fields of individual neurons.
71. Prevedel R, Yoon YG, Hoffmann M, Pak N, Wetzstein G, Kato S, Schrodell T, Raskar R, Zimmer M, Boyden ES, Vaziri A: **Simultaneous whole-animal 3D imaging of neuronal activity using light-field microscopy.** *Nat Methods* 2014, **11**:727-730.
72. Holekamp TF, Turaga D, Holy TE: **Fast three-dimensional fluorescence imaging of activity in neural populations by objective-coupled planar illumination microscopy.** *Neuron* 2008, **57**:661-672.
73. Ahrens MB, Orger MB, Robson DN, Li JM, Keller PJ: **Whole-brain functional imaging at cellular resolution using light-sheet microscopy.** *Nat Methods* 2013, **10**:413-420.
74. Sato TR, Gray NW, Mainen ZF, Svoboda K: **The functional microarchitecture of the mouse barrel cortex.** *PLoS Biol* 2007, **5**:e189.
75. Kerr JN, Greenberg D, Helmchen F: **Imaging input and output of neocortical networks in vivo.** *Proc Natl Acad Sci USA* 2005, **102**:14063-14068.
76. Dombeck DA, Khabbazz AN, Collman F, Adelman TL, Tank DW: **Imaging large-scale neural activity with cellular resolution in awake, mobile mice.** *Neuron* 2007, **56**:43-57.
77. Greenberg DS, Kerr JN: **Automated correction of fast motion artifacts for two-photon imaging of awake animals.** *J Neurosci Methods* 2009, **176**:1-15.
Introduces an algorithm for line-by-line motion correction that is now widely used.
78. Kaifosh P, Zaremba JD, Danielson NB, Losonczy A: **SIMA: Python software for analysis of dynamic fluorescence imaging data.** *Front Neuroinform* 2014, **8**:80.
79. Diego F, Reichneek S, Both M, Hamprecht FA: **Automated identification of neuronal activity from calcium imaging by sparse dictionary learning.** *IS Biomed Imag* 2013:1058-1061.
Presents a promising algorithm for automated segmentation based on dictionary learning. Assumes sparse activity patterns in space and time.
80. Mukamel EA, Nimmerjahn A, Schnitzer MJ: **Automated analysis of cellular signals from large-scale calcium imaging data.** *Neuron* 2009, **63**:747-760.
81. Ji N, Sato TR, Betzig E: **Characterization and adaptive optical correction of aberrations during in vivo imaging in the mouse cortex.** *Proc Natl Acad Sci USA* 2012, **109**:22-27.
82. Scheuss V, Yasuda R, Sobczyk A, Svoboda K: **Nonlinear [Ca2+] signaling in dendrites and spines caused by activity-dependent depression of Ca2+ extrusion.** *J Neurosci* 2006, **26**:8183-8194.
83. Nauhaus I, Nielsen KJ, Callaway EM: **Nonlinearity of two-photon Ca2+ imaging yields distorted measurements of tuning for v1 neuronal populations.** *J Neurophysiol* 2012, **107**:923-936.
84. Yaksi E, Friedrich RW: **Reconstruction of firing rate changes across neuronal populations by temporally deconvolved Ca2+ imaging.** *Nat Methods* 2006, **3**:377-383.
85. Grewe BF, Langer D, Kasper H, Kampa BM, Helmchen F: **High-speed in vivo calcium imaging reveals neuronal network activity with near-millisecond precision.** *Nat Methods* 2010, **7**:399-405.
86. Vogelstein JT, Packer AM, Machado TA, Sippy T, Babadi B, Yuste R, Paninski L: **Fast nonnegative deconvolution for spike train inference from population calcium imaging.** *J Neurophysiol* 2010, **104**:3691-3704.
Introduces an algorithm for deconvolution of fluorescence time series to extract estimates of spiking. This algorithm is widely used.
87. Vogelstein JT, Watson BO, Packer AM, Yuste R, Jedynek B, Paninski L: **Spike inference from calcium imaging using sequential Monte Carlo methods.** *Biophys J* 2009, **97**:636-655.
88. Freeman J, Vladimirov N, Kawashima T, Mu Y, Sofroniew NJ, Bennett DV, Rosen J, Yang CT, Looger LL, Ahrens MB: **Mapping brain activity at scale with cluster computing.** *Nat Methods* 2014, **11**:941-950.
Introduces a library of software tools for analysis of dynamic imaging data by large-scale distributed computing.
89. Freeman J: **Open source technologies for large-scale brain mapping.** *Curr Opin Neurobiol* 2015.
90. Cunningham JP, Yu BM: **Dimensionality reduction for large-scale neural recordings.** *Nat Neurosci* 2014, **17**:1500-1509.
91. Lecoq J, Savall J, Vucinic D, Grewe BF, Kim H, Li JZ, Kitch LJ, Schnitzer MJ: **Visualizing mammalian brain area interactions by dual-axis two-photon calcium imaging.** *Nat Neurosci* 2014, **17**:1825-1829.
Measures activity across two brain areas simultaneously by using two optical paths.
92. Stirman JN, Smith IT, Kudenov MW, Smith SL: **Wide field-of-view, twin-region two-photon imaging across extended cortical networks.** *bioRxiv* 2015 <http://dx.doi.org/10.1101/011320>.